J. Fluid Mech. (1974), *vol.* 63, *part* 3, *pp.* 593–605
Printed in Great Britain

On the stability of a magnetically driven rotating fluid flow

By A. T. RICHARDSON
Department of Engineering Mathematics, University of Bristol

(Received 8 August 1973)

After making the laboratory approximation of small magnetic Reynolds number, the steady, axisymmetric and purely azimuthal velocity profile that in principle can be generated in an incompressible viscous electrically conducting fluid contained in a fixed infinitely long circular cylinder by a magnetic field transverse to the cylinder axis and uniformly rotating with low frequency is subjected to infinitesimal axisymmetric perturbations. The principle of the exchange of stabilities is assumed to hold and the marginal-stability problem becomes a sixth-order eigenvalue problem involving the magnetic Taylor number and the axial wavenumber. An asymptotic analysis, based on the assumption that the magnetic Taylor number is large, and using solutions of the comparison equation $d^6y/dz^6 = zy$, is presented in order to obtain first approximations to the neutral-stability curves of the first and second eigenmodes, and compared with the results of direct numerical integration. It is found that at the onset of instability the secondary motions have a multi-cell structure, the motions in the region, near the cylinder wall, of adversely distributed angular momentum driving through weak viscous action the cells in the interior.

1. Introduction

In the last decade there has been considerable theoretical interest shown in the rotation by electromagnetic methods of liquid metals in cylindrical containers. The use of liquid sodium as a coolant in fast breeder nuclear reactors has created an interest in the possibility of centrifugal gas and particle separation by the rotation of magnetic fields. A description of an electromagnetic rotary-flow generating device, designed to assess the merits of such an idea and based on the experiments of Hobdell & Salzano (1970), has been given by Hayes, Baum & Hobdell (1971). It is in this field that the motivation for the present investigation lies, but similar magnetohydrodynamic configurations are encountered in determining the resistivities of reactive liquid metals and alloys at high temperatures (Ozelton & Wilson 1966; Ayers, Taher & Faux 1971), and in the larger scale induction stirring in the steel manufacturing process (Sundberg 1971; Linder 1971). Large-scale metallurgical applications of this particular branch of magnetohydrodynamics have accounted for the bulk of the published material, both empirical and theoretical, including the prolific contribution of Kapusta and his co-workers in the Soviet Union, that has recently been critically reviewed by Dahlberg (1972).

Moffatt (1965) was the first to construct a mathematical model in which an incompressible electrically conducting viscous fluid contained in a fixed insulating infinitely long circular cylinder is rotated by a magnetic field rotating uniformly in a plane perpendicular to the cylinder axis. Making the laboratory approximation of small magnetic Reynolds number, he showed that if the frequency of rotation of the magnetic field is sufficiently high the fluid can, in principle, rotate as a rigid body inside a viscous boundary layer adjoining the cylinder walls. On the other hand, Smith (1964) determined the cubic nature of the purely azimuthal fluid velocity profile in the somewhat similar problem of a fixed small magnetic field in which the cylinder containing the fluid rotates with small angular velocity. More recently Dahlberg (1972) has shown that for a slightly modified Moffatt model, provided that the magnetic field strength is sufficiently small to ensure the validity of the laboratory approximation, a steady, axisymmetric and purely azimuthal velocity profile can be generated by rotating the field at any frequency. Furthermore, as is to be expected from the skin effect, for fixed field strength, the Moffatt rigid-body angular velocity decreases as the rotation frequency of the field becomes very large.

From the practical point of view of a centrifuge it is important to know whether or not a state of laminar azimuthal motion could be maintained. Indeed, both the low frequency and high frequency velocity profiles may become unstable and secondary motions develop before significant magnetic field strengths and rotation frequencies are reached. Whether the model describes a centrifuge or a mixer depends of course on its stability characteristics. Kapusta, Dremov & Bartoshuk (1971) have attempted a linear stability analysis of the low frequency profile. However, Dahlberg (1972) has cast doubt on their methods of analysis. It is the aim of this paper to determine the onset of instability, when the low frequency model is subjected to infinitesimal axisymmetric disturbances, and to describe the consequent secondary motions using an asymptotic analysis to support the results of direct numerical integration of the perturbation equations.

2. The linear stability problem

2.1. *The equilibrium configuration*

Suppose that an incompressible fluid of constant density ρ, kinematic viscosity ν and electrical conductivity σ is contained in the interior ($r < a$) of a fixed insulating cylindrical container whose inner and outer boundaries correspond to $r = a$ and $r = \lambda a$ ($\lambda > 1$), respectively, in cylindrical polar co-ordinates (r, θ, z). A magnetic field is applied perpendicular to the cylinder axis and is made to rotate with uniform angular velocity ω. The source of this field can be idealized by longitudinal surface currents at $r = \lambda a$, regarded perhaps as the inner surface of a stator, and then the magnetic field $\mathbf{B}$ can satisfy

$$B_\theta(\lambda a-, \theta, z) = B_0 \cos(\theta - \omega t), \quad B_z(r, \theta, z) = 0 \quad (0 \leqslant r < \lambda a). \tag{2.1}$$

The exterior region $r > \lambda a$ is assumed to have infinite magnetic permeability μ and so have no effect on the inner region $r \leqslant \lambda a$.

The effect of the rotating magnetic field is to induce currents in the conducting fluid and so create a Lorentz force that will generate fluid motion. A dimensional analysis of the problem indicates that there must be three non-dimensional numbers that quantify the applied magnetic field strength and the rotation frequency and specify the particular fluid being rotated. For convenience the Hartmann number M, a 'second' magnetic Reynolds number R_m^* and the magnetic Prandtl number p_m, defined by

$$M = aB_0(\sigma/\rho\nu)^{\frac{1}{2}}, \quad R_m^* = a^2\omega/\eta, \quad p_m = \nu/\eta, \tag{2.2}$$

where $\eta = (\mu\sigma)^{-1}$ denotes the electrical resistivity, will be chosen. Once these three quantities have been specified the fluid velocity $\mathbf{u}$ and the magnetic field $\mathbf{B}$ can, in principle, be obtained from the governing magnetohydrodynamic equations:

$$\rho\left(\frac{\partial \mathbf{u}}{\partial t}+\mathbf{u}.\nabla\mathbf{u}\right) = -\nabla p+\frac{1}{\mu}\nabla\times\mathbf{B}\times\mathbf{B}-\rho\nu\nabla\times\nabla\times\mathbf{u}, \tag{2.3}$$

$$\partial\mathbf{B}/\partial t = \nabla\times(\mathbf{u}\times\mathbf{B})-\eta\nabla\times\nabla\times\mathbf{B} \quad (r < a), \tag{2.4}$$

$$\nabla\times\mathbf{B} = 0 \quad (a < r < \lambda a), \tag{2.5}$$

$$\nabla.\mathbf{u} = 0, \quad [\nabla.\mathbf{B} = 0], \tag{2.6}$$

in a fixed laboratory reference frame, where p denotes the kinetic pressure and mks units have been used.

Let $\mathscr{U}$ denote a typical fluid velocity. Then the ordinary magnetic Reynolds number

$$R_m = \mathscr{U}a/\eta \tag{2.7}$$

is a measure of the relative importance of the induction and diffusion terms in (2.4). In the laboratory R_m is small and neglecting the effect of the fluid motions on the magnetic field decouples the Navier–Stokes and induction equations. By solving for $\mathbf{B} = (B_r, B_\theta, 0)$, ensuring continuity with the potential field in the insulator and noting that the curl of the Lorentz force is independent of θ and t, Dahlberg (1972) shows that the fluid velocity can be purely azimuthal and given by

$$u_\theta = \frac{M^2\omega r}{16|D|^2}\sum_{n=0}^{\infty}\frac{[1-(r/a)^{4n+2}]\,(\frac{1}{4}R_m^*)^{2n}}{(2n+1)\,(2n+1)\,!\,[(n+1)\,!]^2}, \tag{2.8a}$$

$$\simeq \frac{M^2\omega r}{16|D|^2}[1-(r/a)^2+O(R_m^{*2})], \tag{2.8b}$$

where $|D|$ denotes the modulus of the complex quantity

$$D = J_0\{(iR_m^*)^{\frac{1}{2}}\}-\lambda^{-2}J_2\{(iR_m^*)^{\frac{1}{2}}\} \tag{2.9}$$

and J_n is the Bessel function of the first kind of order n. This result depends crucially on the assumptions of z independence and $R_m \ll 1$, this latter condition necessarily imposing a restriction on the magnitude of the magnetic field. The stability of the cubic velocity profile [cf. (2.8*b*) and (2.9)] resulting from the assumption of small R_m^* is discussed in the remaining sections.

2.2. *The axisymmetric perturbation equations and boundary conditions*

Let $\mathbf{u}$, $\delta\mathbf{B}$ and $\rho\varpi$ be perturbations, whose squares and products are negligible, in the velocity, magnetic field and kinetic pressure respectively of the two-dimensional equilibrium state with azimuthal velocity [cf. (2.8*b*)]

$$V(r) = \tfrac{1}{16}M^2\omega r[1-(r/a)^2]. \tag{2.10}$$

Having made the approximation $R_m \ll 1$, the magnetic perturbation must satisfy

$$(\partial/\partial t+\eta\nabla\times\nabla\times)\,\delta\mathbf{B} = 0 \quad (0 \leqslant r < a), \tag{2.11a}$$

$$\nabla\times\delta\mathbf{B} = 0 \quad (a < r < \lambda a), \tag{2.11b}$$

$$\nabla\,.\,\delta\mathbf{B} = 0, \tag{2.12}$$

being continuous across the boundary $r = a$, and if the magnetic field components B_θ and B_z at $r = \lambda a$ retain their equilibrium values [cf. (2.1)] it is easily seen that

$$\delta\mathbf{B} = 0 \quad (0 \leqslant r < \lambda a), \tag{2.13}$$

from which it immediately follows that $\delta(\nabla\times\mathbf{B}\times\mathbf{B}/\mu)$, the perturbation in the Lorentz force, vanishes throughout the fluid. As Moffatt (1965) has pointed out, the linear stability problem is then a fluid-dynamic one since the role of the magnetic field to this order is to establish the equilibrium profile.

The linearized Navier–Stokes equations governing axisymmetric disturbances are

$$\frac{\partial u_r}{\partial t}-\frac{2Vu_\theta}{r} = -\frac{\partial\varpi}{\partial r}+\nu\left(\nabla^2 u_r-\frac{u_r}{r^2}\right), \tag{2.14}$$

$$\frac{\partial u_\theta}{\partial t}+\left(\frac{dV}{dr}+\frac{V}{r}\right)u_r = \nu\left(\nabla^2 u_\theta-\frac{u_\theta}{r^2}\right), \tag{2.15}$$

$$\frac{\partial u_z}{\partial t} = -\frac{\partial\varpi}{\partial z}+\nu\nabla^2 u_z, \tag{2.16}$$

where
$$\nabla^2 = \frac{\partial^2}{\partial r^2}+\frac{1}{r}\frac{\partial}{\partial r}+\frac{\partial^2}{\partial z^2}, \tag{2.17}$$

and the continuity equation reduces to

$$\frac{\partial u_r}{\partial r}+\frac{u_r}{r}+\frac{\partial u_z}{\partial z} = 0. \tag{2.18}$$

If the perturbations are analysed into normal modes so that

$$\left.\begin{aligned} u_r &= F(r)\cos(kz)\,e^{pt}, & u_\theta &= G(r)\cos(kz)\,e^{pt},\\ u_z &= H(r)\sin(kz)\,e^{pt}, & \varpi &= W(r)\cos(kz)\,e^{pt},\end{aligned}\right\} \tag{2.19}$$

where k is an axial wavenumber and p is a frequency that can be complex, then substitution into (2.14)–(2.16) and (2.18) and elimination of W gives

$$\left(DD_*-k^2-\frac{p}{\nu}\right)(DD_*-k^2)\,F = \frac{2k^2}{\nu r}VG, \tag{2.20}$$

$$\left(DD_* - k^2 - \frac{p}{\nu}\right) G = \frac{(D_* V) F}{\nu}, \tag{2.21}$$

$$kH = -D_* F, \tag{2.22}$$

where
$$D = \frac{d}{dr}, \quad D_* = \frac{d}{dr} + \frac{1}{r}. \tag{2.23}$$

Introducing the non-dimensional variables

$$x = r/a, \quad \alpha = ka, \quad q = pa^2/\nu, \tag{2.24}$$

and assuming that the principle of the exchange of stabilities is valid, the marginal-stability equations governing F and G become

$$(DD_* - \alpha^2)^2 F = \alpha^2 T_m^{\frac{1}{2}} (1 - x^2)\, G, \tag{2.25}$$

$$(DD_* - \alpha^2)\, G = T_m^{\frac{1}{2}} (1 - 2x^2)\, F, \tag{2.26}$$

where T_m is a magnetic Taylor number defined by

$$T_m^{\frac{1}{2}} = \frac{M^2 a^2 \omega}{8\nu} = \frac{M^2 R_m^*}{8 p_m} = \frac{\omega a^4 B_0^2}{8\mu\rho\nu^2\eta}, \tag{2.27}$$

and D and D_* now denote derivatives with respect to x.

With fixed wavenumber α and a set of six boundary conditions, (2.25) and (2.26) constitute a sixth-order linear eigenvalue problem for T_m, and as in other problems of hydrodynamic stability, the appearance of ν^{-4} in the definition of the magnetic Taylor number suggests that T_m can be considered as a large parameter. At the fluid–solid insulator boundary $x = 1$ clearly the no-slip conditions must be satisfied, so that

$$F = DF = G = 0 \quad \text{at} \quad x = 1. \tag{2.28}$$

However, the exact nature of the boundary conditions to be applied at $x = 0$ is not immediately apparent. In order to clarify this situation, the form of the solutions near $x = 0$ can be determined on the assumption that $T_m^{\frac{1}{4}}$ is large and α is of order unity. Defining the scaled variable

$$y = \alpha^{\frac{1}{2}} T_m^{\frac{1}{4}} x, \tag{2.29}$$

equations (2.25) and (2.26), to leading order, become

$$(DD_*)^2 F = 0, \quad DD_* G = F/\alpha, \tag{2.30}$$

respectively, having general solution

$$F = 2\alpha[(4A_2 + 3A_6)\, y + 12 A_3 y^3 + A_5/y + 4A_6 y \ln y], \tag{2.31}$$

$$G = A_1 y + A_2 y^3 + A_3 y^5 + A_4/y + A_5 y \ln y + A_6 y^3 \ln y, \tag{2.32}$$

where the A_i ($i = 1, 2, \ldots, 6$) are arbitrary constants. At $x = 0$ (i.e. $y = 0$) the azimuthal velocity component must vanish by symmetry, implying that $A_4 = 0$. A finite and in fact zero radial velocity at $x = 0$ implies that $A_5 = 0$, and symmetry of the axial velocity, so that $DH = 0$, implies that $A_6 = 0$. These restrictions on F and G are equivalent to

$$F = D^2 F = G = 0 \quad \text{at} \quad x = 0. \tag{2.33}$$

Hence (2.25) and (2.26) together with boundary conditions (2.28) and (2.33) constitute the axisymmetric linear stability problem, and in the following section an asymptotic analysis is presented on the assumption that the magnetic Taylor number is large.

3. Asymptotic analysis

3.1. *WKBJ solutions and comparison equations*

If approximate solutions of the form

$$[F, G] = [f(x, T_m^{-\frac{1}{2}}), g(x, T_m^{-\frac{1}{2}})] \exp[\pm i\alpha^{\frac{1}{3}} T_m^{\frac{1}{6}} S(x)], \tag{3.1}$$

where f and g are analytic functions of x and $T_m^{-\frac{1}{2}}$, α is of order unity and $T_m^{\frac{1}{6}}$ is a large parameter, are sought to (2.25) and (2.26), then the leading-order equations obtained after substitution imply that the function $S(x)$ must satisfy

$$(DS)^6 = (1-x^2)(2x^2-1). \tag{3.2}$$

As a result, there are clearly four transition points of the governing differential equations, but only those at $x = 1/\sqrt{2}$ and $x = 1$ are of direct physical relevance. On passing through $x = 1/\sqrt{2}$ the character of the solution (3.1) changes since the right-hand side of (3.2) changes sign. On the other hand, the transition point at $x = 1$ corresponds to the fluid–solid insulator boundary and so has a different role to play in the determination of the final solution. The underlying physical significance of these points is apparent on considering the Rayleigh discriminant, which for the velocity profile (2.10) is

$$\Phi(x) = -\tfrac{1}{64} M^4 \omega^2 a^3 x^3 (1-x^2)(2x^2-1). \tag{3.3}$$

Then, in the range $1/\sqrt{2} < x < 1$, $S(x)$ can take real values [cf. (3.2)] and $\Phi(x)$ takes negative values, indicating that the region is one of adverse distribution of angular momentum, and therefore of possible dynamical instability.

If the nature of the solution to (2.25) and (2.26) as it passes through $x = 1/\sqrt{2}$, having satisfied the boundary conditions at $x = 0$, is determined and then matched with a suitable linear combination of solutions (3.1), $S(x)$ will be effectively specified. However, it will be found that only for a discrete set of values of $\alpha^2 T_m$ will this combination match with the solution satisfying the no-slip conditions at $x = 1$. The resulting estimates of $\alpha^2 T_m$ will then provide a valuable comparison with the numerically determined neutral-stability curves.

In order to examine the behaviour of the solutions in the vicinity of the transition points define

$$\xi = (1/\sqrt{2} - x)/\epsilon, \quad \epsilon = (2\alpha^4 T_m^2)^{-\frac{1}{14}}, \tag{3.4}$$

$$\zeta = (x-1)/\epsilon^*, \quad \epsilon^* = (2\alpha^2 T_m)^{-\frac{1}{7}}. \tag{3.5}$$

Then to the leading order in ϵ and ϵ^* equations (2.25) and (2.26) become

$$D^6 F = \xi F, \quad D^2 G = \zeta G \tag{3.6}$$

respectively. The comparison equation is the same for both cases, and therefore an examination of the solutions of $D^6 F = zF$ for both large and small moduli of the complex variable z must be made.

3.2. *Solutions in the vicinity of the transition points*

Using an argument involving Laplace integrals (cf. Duty & Reid 1964; Granoff & Bleistein 1972) the differential equation $D^6F = zF$ can be shown to have contour-integral solutions of the form

$$F_j(z) = \frac{1}{2\pi i}\int_{\Gamma_j} e^{zs-\frac{1}{7}s^7}\,ds \quad (j = 1, 2, \ldots, 7), \tag{3.7}$$

where the Γ_j are infinite contours in the complex-s plane with end points in the 'valleys' of $-s^7$, given by

$$\tfrac{2}{7}n\pi - \tfrac{1}{14}\pi < \arg s < \tfrac{2}{7}n\pi + \tfrac{1}{14}\pi \quad (n = 0, 1, \ldots, 6). \tag{3.8}$$

However, only six of these solutions are linearly independent since

$$\sum_{j=1}^{7} F_j(z) = 0,$$

and these are related since

$$F_{j+1}(z) = e^{\frac{2}{7}\pi i}F_j(z\,e^{\frac{2}{7}\pi i}) \quad (j = 1, 2, \ldots, 6).$$

It is a relatively straightforward matter, using the method of steepest descents, to obtain the leading term in an expansion of $F_j(z)$ for large $|z|$. If Γ_1 is chosen to be a path lying in the sector $\frac{6}{7}\pi < \arg s < \frac{8}{7}\pi$, and a cut is inserted along $\arg z = \frac{10}{7}\pi$, $F_1(z)$ has the asymptotic behaviour

$$F_1(z) \sim \begin{cases} -[2(3\pi)^{\frac{1}{2}}]^{-1} z^{-\frac{5}{12}} \exp(-\frac{6}{7}z^{\frac{7}{6}}) \quad \text{for} \quad -\frac{4}{7}\pi < \arg z < \frac{6}{7}\pi, & (3.9a) \\ -[2(3\pi)^{\frac{1}{2}}]^{-1} z^{-\frac{5}{12}} \exp[\frac{5}{6}\pi i - \frac{6}{7}z^{\frac{7}{6}} \exp(-\frac{1}{3}i\pi)] & \\ \qquad\qquad \text{for} \quad \frac{8}{7}\pi < \arg z < \frac{10}{7}\pi & (3.9b) \end{cases}$$

(cf. Duty & Reid 1964).

The physical problem requires that for z real and positive and equal to ξ only decaying solutions are acceptable. From expressions (3.9) the asymptotic behaviour of the remaining solutions can be determined, and it is found that the only solutions becoming exponentially small as $\xi \to \infty$, all others becoming unbounded, are F_1, F_2 and F_7. Hence the required solution, without loss of generality, can be written as the linear combination $F = F_1 + \beta_2 F_2 + \beta_7 F_7$. The whole point of this analysis is to determine the behaviour of this solution as $\xi \to -\infty$; i.e. with z lying on the negative real axis. Since F_4 and F_5 both tend to zero and F_3 and F_6 are bounded as $\xi \to -\infty$, the constants β_2 and β_7 must be chosen so that the exponentially large contribution to $F_1 = -F_2 - F_3 - F_4 - F_5 - F_6 - F_7$ in the sector $\frac{6}{7}\pi < \arg z < \frac{8}{7}\pi$ is removed. Choosing $\beta_2 = \beta_7 = 1$ then gives

$$F \propto (-\xi)^{-\frac{5}{12}} \cos[\tfrac{6}{7}(-\xi)^{\frac{7}{6}} - \tfrac{1}{4}\pi] \quad \text{as} \quad \xi \to -\infty, \tag{3.10}$$

and this provides one of the boundary conditions on the WKBJ solution (3.1).

As already mentioned, the problem in the vicinity of $x = 1$ is slightly different from that in the vicinity of $x = 1/\sqrt{2}$. The asymptotic solution for large negative z equal to ζ [cf. definition (3.5)] must be linked with the series solution about $\zeta = 0$ that satisfies the no-slip conditions. Now for large and negative z lying in the sector $\frac{6}{7}\pi < \arg z < \frac{8}{7}\pi$ only a bounded oscillatory linear combination of the functions $F_j(z)$ is acceptable. Without loss of generality, G can then be written in the form $G = \beta_3 F_3 + \beta_4 F_4 + \beta_5 F_5 + F_6$, and from the leading-order equations after making the substitutions (3.5), the no-slip boundary conditions (2.28) are readily shown to be equivalent to

$$G = D^2 G = D^3 G = 0 \quad \text{at} \quad \zeta = 0. \tag{3.11}$$

In order to apply these conditions (3.11) consider the functions $q_j(z)$ defined by

$$q_j(z) = \frac{1}{2\pi i}\int_0^\infty e^{zs - \frac{1}{7}s^7}\, ds \quad (j = 0, 1, \ldots, 6), \tag{3.12}$$

where the path of integration is the semi-infinite ray given by $\arg s = \frac{2}{7}\pi j$. Although these functions individually do not satisfy $D^6 F = zF$, certain combinations of them obviously do, for example, $q_4(z) - q_3(z) = F_1(z)$ [cf. (3.7)]. After noting that the functions $q_j(z)$ are related in the same way as are the solutions $F_j(z)$, expanding $q_j(z)$ in an ascending power series in z and observing that $q_0(0)$ and its derivatives $q_0''(0)$ and $q_0'''(0)$ are non-zero quantities, the boundary conditions (3.11) provide three linear algebraic equations for β_3, β_4 and β_5 whose solution is

$$\beta_3 = -e^{\frac{2}{7}\pi i}, \quad \beta_4 = 1 + e^{\frac{8}{7}\pi i} + e^{\frac{10}{7}\pi i}, \quad \beta_5 = -e^{\frac{2}{7}\pi i} - e^{\frac{6}{7}\pi i} - e^{\frac{8}{7}\pi i}. \tag{3.13}$$

Since F_4 and F_5 are exponentially small for z large and negative, the resulting linear combination then indicates a solution of the form

$$G \propto (-\zeta)^{-\frac{5}{12}} \cos\left[\tfrac{6}{7}(-\zeta)^{\frac{7}{6}} + \tfrac{11}{28}\pi\right] \quad \text{as} \quad \zeta \to -\infty, \tag{3.14}$$

which constitutes the second boundary condition on the WKBJ solution (3.1).

3.3. *Approximations to neutral-stability curves*

Since the function $S(x)$ in the exponent of solutions (3.1) is required to take real values in the range $1/\sqrt{2} \leqslant x \leqslant 1$ define

$$S(x) = \int_{1/\sqrt{2}}^{x} [(1 - x^2)(2x^2 - 1)]^{\frac{1}{6}}\, dx + B, \tag{3.15}$$

where B is an arbitrary constant. Then expanding $S(x)$ in ascending powers of $x - 1/\sqrt{2}$ and $1 - x$ and using definitions (3.4) and (3.5) to express the leading term in the inner variables ξ and ζ respectively gives

$$\alpha^{\frac{1}{3}} T_m^{\frac{1}{6}} S(x) \simeq \begin{cases} \frac{6}{7}(-\xi)^{\frac{7}{6}} + B\alpha^{\frac{1}{3}} T_m^{\frac{1}{6}}, & (3.16a) \\ (I + B)\,\alpha^{\frac{1}{3}} T_m^{\frac{1}{6}} - \frac{6}{7}(-\zeta)^{\frac{7}{6}}, & (3.16b) \end{cases}$$

where
$$I = \int_{1/\sqrt{2}}^{1} [(1 - x^2)(2x^2 - 1)]^{\frac{1}{6}}\, dx \simeq 0{\cdot}18834. \tag{3.17}$$

If a solution of the form

$$F(x) \propto \cos\left[\alpha^{\frac{1}{3}} T_m^{\frac{1}{6}} S(x)\right] \tag{3.18}$$

is sought, the leading-order equations of the large-T_m approximation to (2.25) and (2.26) indicate that $G(x)$ also has this form. Now matching at $x = 1/\sqrt{2}+$ using (3.10), (3.16) and (3.18) determines the constant B, so that

$$\alpha^{\frac{1}{3}} T_m^{\frac{1}{6}} B = -\tfrac{1}{4}\pi. \tag{3.19}$$

On the other hand, since (3.14) and (3.18) are proportionality relations, in the matching at $x = 1-$ the identity

$$\cos\theta = (-1)^m \cos(m\pi - \theta), \tag{3.20}$$

where m is an integer, must be used. The lowest positive value that $\alpha^{\frac{1}{3}}T_m^{\frac{1}{6}}$ can take is obtained from (3.14), (3.18) and (3.20) with $m = 1$, and the resulting approximation to the neutral-stability curve for the first axisymmetric mode is

$$\alpha^{\frac{1}{3}}T_m^{\frac{1}{6}} = 6\pi/7I \quad \text{or} \quad \alpha^2 T_m \simeq 8{\cdot}5416 \times 10^6. \tag{3.21}$$

Similarly, from (3.20) with $m = 2$, the approximation to the neutral-stability curve of the second axisymmetric mode is

$$\alpha^{\frac{1}{3}}T_m^{\frac{1}{6}} = 13\pi/7I \quad \text{or} \quad \alpha^2 T_m \simeq 8{\cdot}8367 \times 10^8. \tag{3.22}$$

These curves are compared with those obtained by direct numerical integration of the marginal-stability equations in figures 1 and 2.

4. Numerical results

The eigenvalue problem defined by (2.25), (2.26), (2.28) and (2.33) is a two-point boundary-value problem and was solved by using a Chebyshev collocation method in which F and G are each represented by a finite series of Chebyshev polynomials. For a discussion of the basic principles of such a technique see Wright (1964) and Hurley, Roberts & Wright (1966). However, the essence of the method is the production of a set of linear algebraic equations for the unknown coefficients of the Chebyshev series so that the whole differential boundary-value problem can be solved in one step.

To avoid obtaining the trivial solution $F = G = 0$, a normalization condition $F = 1$ at $x = 0{\cdot}5$ was substituted for the correct boundary condition $F = 0$ at $x = 1$. Then for a specified wavenumber α and an initial estimate of the magnetic Taylor number T_m [cf. (3.21) and (3.22)] the modified problem was solved and the in general non-zero value of F at $x = 1$ obtained. The omitted condition was then used as a discriminant, and by approaching iteratively its first two positive zeros successive converging estimates of T_m were derived.

Calculations were performed using double-precision arithmetic on an ICL System 4–75 machine. Because of the nature of the resulting eigenfunctions it was found necessary to use polynomial approximations of degree at least 20. For a specific wavenumber α the iteration was terminated as soon as either the magnetic Taylor number or discriminant differed from its previous value by not more than 10^{-7}. However, in practice, the actual difference was much smaller than this, as indeed was the magnitude of the discriminant. The results obtained for the first mode, using approximating polynomials of degree 20, were then checked by verifying that the last terms in the Chebyshev series were small, and by repeating the calculation with polynomials of degree 25. The corresponding magnetic Taylor number confirmed the significance of the first six digits. Higher order approximations gave further confirmation and were indeed considered necessary for the determination of the second mode.

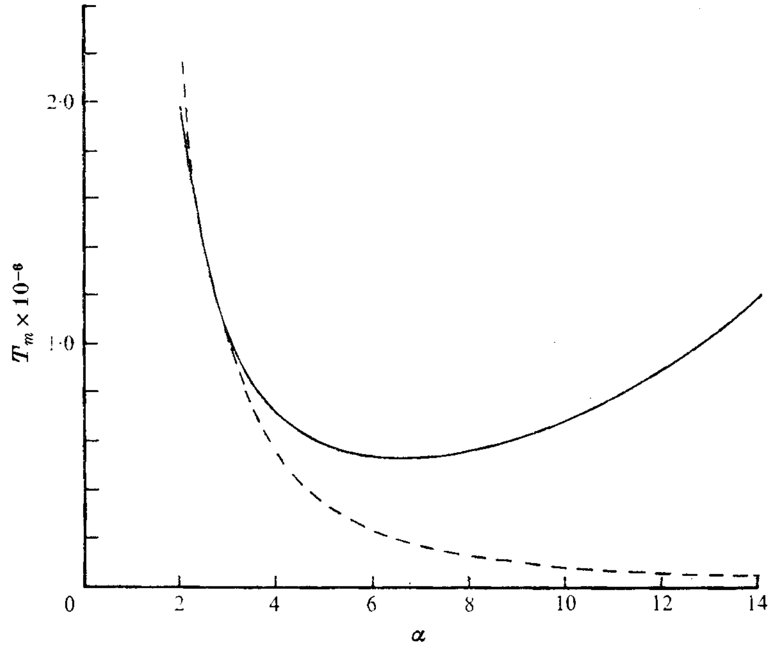

FIGURE 1. The numerically calculated neutral-stability curve for the first mode (full line) and its approximation using the asymptotic analysis (broken line).

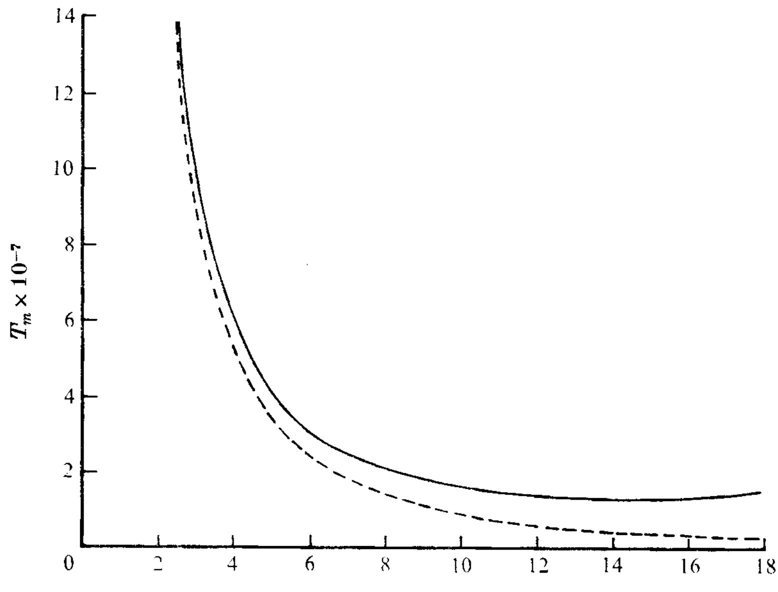

FIGURE 2. The numerically calculated neutral-stability curve for the second mode (full line) and its approximation using the asymptotic analysis (broken line).

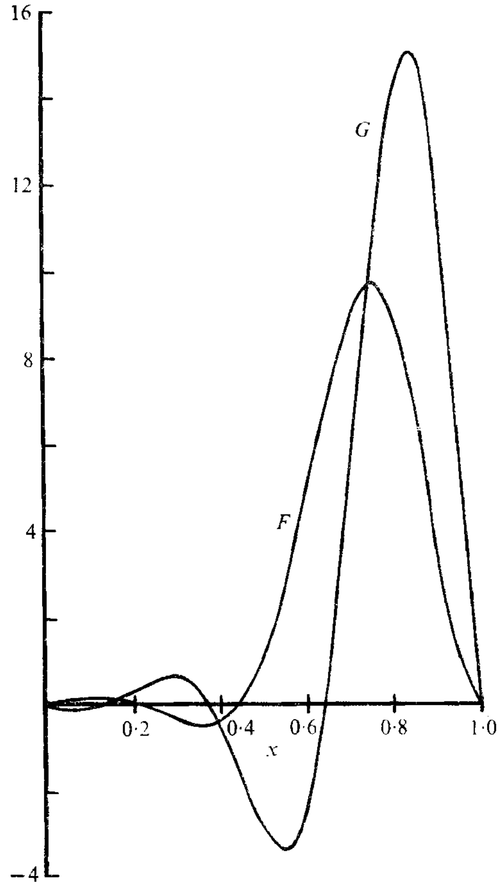

FIGURE 3. The amplitudes of the radial eigenfunction F and azimuthal eigenfunction G of the first mode, normalized so that $F = 1$ at $x = 0{\cdot}5$, at the onset of instability, for which $T_{mc} \simeq 531\,811$ and $\alpha_c \simeq 6{\cdot}59$.

Repeating this procedure for various values of α produced the neutral-stability curves for the first and second axisymmetric modes of instability illustrated in figures 1 and 2. The critical values of the magnetic Taylor number and wave-number at the onset of instability for the first mode were then found to be

$$T_{mc} \simeq 531\,811, \quad \alpha_c \simeq 6{\cdot}59, \tag{4.1}$$

and for the second mode

$$T_{mc} \simeq 1{\cdot}381 \times 10^7, \quad \alpha_c \simeq 14{\cdot}5. \tag{4.2}$$

The corresponding eigenfunctions for the first mode are illustrated in figure 3. Of particular interest is the form of the radial eigenfunction since this is proportional to the stream function that describes motion in planes through the cylinder axis. There are therefore three cells, the largest of which extends over half of the cylindrical region including the region predicted by Rayleigh's criterion [cf. (3.3)] to be dynamically unstable. The other two cells are then viscously driven in a dynamically stable region and consequently have small amplitudes. In

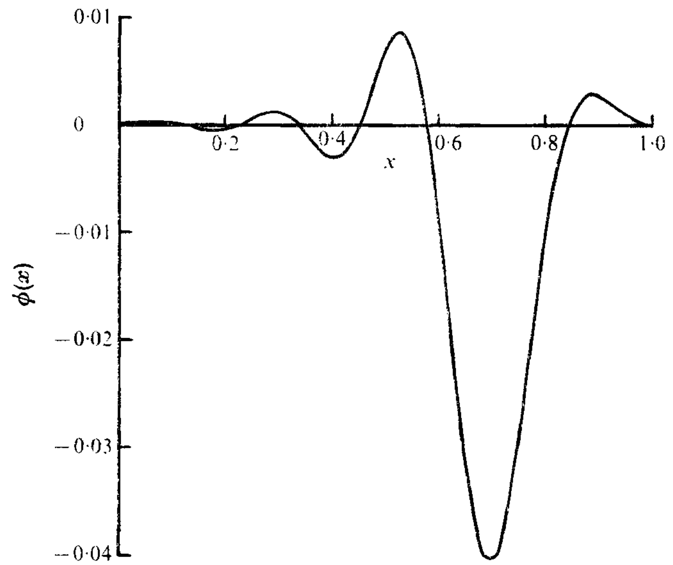

FIGURE 4. The function $\phi(x) = e^{-10x}F(x)$ for the second mode, normalized so that the amplitude of the radial eigenfunction $F = 1$ at $x = 0{\cdot}5$, at the onset of instability, for which $T_{mc} \simeq 1{\cdot}381 \times 10^7$ and $\alpha_c \simeq 14{\cdot}5$.

figure 4 the radial eigenfunction for the second mode is represented and indicates a seven-cell structure, the relatively small amplitudes of the inner cells being particularly apparent.

5. Concluding remarks

First, although the asymptotic analysis presented in § 3 is based on the assumption that $\alpha^{\frac{1}{3}}T_m^{\frac{1}{6}}$ is large, while α is of the order unity, and the resulting estimates (3.21) and (3.22) indicate that $\alpha^{\frac{1}{3}}T_m^{\frac{1}{6}} \simeq 14{\cdot}297$ and $30{\cdot}978$ respectively, these values are sufficiently large for the method to aid and confirm at least some of the numerical calculations.

Second, the velocity profile (2.10), whose stability has been investigated, was derived after making the laboratory approximation $R_m \ll 1$. Taking $\mathscr{U}$, the typical velocity in the definition of the magnetic Reynolds number [cf. (2.7)], as the maximum velocity implies that, for consistency,

$$M^2R_m^* \ll 24\sqrt{3}. \tag{5.1}$$

On the other hand, the numerical analysis suggests that instability may occur if the condition

$$M^2R_m^* \leqslant 729{\cdot}25p_m \tag{5.2}$$

is violated. Taking $p_m = 1{\cdot}51 \times 10^{-7}$ for mercury at 20 °C, condition (5.2) becomes $M^2R_m^* \leqslant 8{\cdot}8 \times 10^{-4}$, indicating that in principle secondary flows could develop as a result of the adverse angular momentum distribution of the primary flow (2.10). However, if the cylinder radius $a = 0{\cdot}03\,\text{m}$, $\rho = 1{\cdot}36 \times 10^4\,\text{kg/m}^3$,

$\sigma = 1{\cdot}05 \times 10^6\,\mathrm{S/m}$, $\nu = 1{\cdot}14 \times 10^{-7}\,\mathrm{m^2/s}$, and $\eta = 7{\cdot}58 \times 10^{-1}\,\mathrm{m^2/s}$ condition (5.2) becomes

$$\omega B^2 \leqslant 1{\cdot}22 \times 10^{-6}, \tag{5.3}$$

if the angular frequency ω is measured in rad/s and the magnetic field strength B in tesla. If liquid sodium at 100 °C is the working fluid then $M^2 R_m^* \leqslant 5{\cdot}6 \times 10^{-2}$, implying that $\omega B^2 \leqslant 4{\cdot}57 \times 10^{-8}$. In both cases, since $\omega \simeq 100\pi$ rad/s in most applications, instability can occur at very small magnetic field strengths. Moreover, finite end-effects, neglected here, could be expected to enhance any secondary flow, and there is still the possibility that the axisymmetric modes are not the most unstable, thus restricting even further the applicability of the two-dimensional equilibrium low frequency theory to practical situations.

I am very grateful to Professor P. H. Roberts for suggesting the asymptotic analysis presented above, and to Dr R. F. Burbidge for his valuable criticisms throughout the development of this work.

REFERENCES

Ayers, R. D., Taher, S. M. A. & Faux, R. L. 1971 *J. Phys.* **E4**, 441.

Dahlberg, E. 1972 *AB Atomenergi, Sweden, Rep.* AE-447.

Duty, R. L. & Reid, W. H. 1964 *J. Fluid Mech.* **20**, 81.

Granoff, B. & Bleistein, N. 1972 *SIAM J. Math. Anal.* **3**, 45.

Hayes, D. J., Baum, M. R. & Hobdell, M. R. 1971 *J. Br. Nucl. Energy Soc.* **10**, 93.

Hobdell, M. R. & Salzano, F. J. 1970 *Nucl. Appl. Tech.* **8**, 95.

Hurley, M., Roberts, P. H. & Wright, K. 1966 *Astrophys. J.* **143**, 535.

Kapusta, A. B., Dremov, V. V. & Bartoshuk, E. S. 1971 *Magn. Gidrodin.* **4**, 31 (in Russian).

Linder, S. 1971 *A.S.E.A. J.* **44**, 83.

Moffatt, H. K. 1965 *J. Fluid Mech.* **22**, 521.

Ozelton, M. W. & Wilson, J. R. 1966 *J. Sci. Instrum.* **43**, 359.

Smith, P. 1964 *Z. angew Math. Mech.* **44**, 495.

Sundberg, Y. 1971 *A.S.E.A. J.* **44**, 71.

Wright, K. 1964 *Comp. J.* **6**, 358.